Monitoring COVID-19 transmission risks by RT-PCR tracing of droplets in hospital and living environments

Andrea Piana[a], Maria Eugenia Colucci[b], Federica Valeriani[c], Adriano Marcolongo[d], Giovanni Sotgiu[a], Cesira Pasquarella[b], Lory Marika Margarucci[c], Andrea Petrucca[d], Gianluca Gianfranceschi[c], Sergio Babudieri[a], Pietro Vitali[b], Giuseppe DôErmo[e], Assunta Bizzarro[b], Flavio De Maio[f], Matteo Vitali[g], Antonio Azara[a], Ferdinando Romano[g], Maurizio Simmaco[e], Vincenzo Romano Spica[c*]

[a] Department of Medical, Surgical and Experimental Sciences, University of Sassari, Viale San Pietro, 43, 07100 Sassari, Italy. (piana@uniss.it; gsotgiu@uniss.it; babuder@uniss.it, azara@uniss.it)

[b] Department of Medicine and Surgery, University Hospital, University of Parma, Via Gramsci, 14, 43126, Parma, Italy (cesiraisabellamaria.pasquarella@unipr.it; mariaeugenia.colucci@unipr.it; assunta.bizzarro@unipr.it; pvitali@ao.pr.it)

[c] Department of Movement, Human and Health Sciences, Unit of Public Health-Laboratory of Epidemiology and Biotechnologies, University of Rome ñForo Italicoò, Piazza Lauro de Bosis 6, 00135 Rome, Italy (vincenzo.romanospica@uniroma4.it; federica.valeriani@uniroma4.it; l.margarucci@studenti.uniroma4.it; gianluca.gianfranceschi@uniroma4.it)

[d] SantôAndrea Hospital, Sapienza University of Rome, Rome, Italy (maurizio.simmaco@uniroma1.it; andrea_petrucca@yahoo.com; marcolongo@ospedalesantandrea.it)

[e] Department of Surgery, Sapienza University of Rome, Rome, Italy (giuseppe.dermo@uniroma1.it)

[f] Dipartimento di Scienze biotecnologiche di base, cliniche intensivologiche e perioperatorie ï Sezione di Microbiologia, Università Cattolica del Sacro Cuore, Rome, Italy, (flavio.demaio@unicatt.it)

[g] Department of Public Health and Infectious Diseases, University of Rome La Sapienza, Rome, Italy (matteo.vitali@uniroma1.it; ferdinando.romano@uniroma1.it)

*Corresponding: Vincenzo Romano Spica; Laboratory of Department of Movement, Human and Health Sciences; University of Rome ñForo Italicoò, Piazza Lauro De Bosis 6, 00135 Rome, Italy, E-mail: vincenzo.romanospica@uniroma4.it

Keywords: SARS-CoV-2; Environmental contamination; Fomite; Droplets; Biological fluids; Microbiota. **Running:** COVID-19 and droplets contamination

ABSTRACT

SARS-CoV-2 environmental contamination occurs through droplets and biological fluids released in the surroundings from patients or asymptomatic carriers. Surfaces and objects contaminated by saliva or nose secretions represent a risk for indirect transmission of COVID-19. We assayed surfaces from hospital and living spaces to identify the presence of viral RNA and the spread of fomites in the environment. Anthropic contamination by droplets and biological fluids was monitored by detecting the microbiota signature using multiplex RT-PCR on selected species and massive sequencing on 16S-amplicons.

A total of 92 samples (flocked swab) were collected from critical areas during the pandemic, including indoor (3 hospitals and 3 public buildings) and outdoor surfaces exposed to anthropic contamination (handles and handrails, playgrounds). Traces of biological fluids were frequently detected in spaces open to the public and on objects that are touched with the hands (>80%). However, viral RNA was not detected in hospital wards or other indoor and outdoor surfaces either in the air system of a COVID-hospital, but only in the surroundings of an infected patient, in consistent association with droplets traces and fomites. Handled objects accumulated the highest level of multiple contaminations by saliva, nose secretions and faecal traces, further supporting the priority role of handwashing in prevention.

In conclusion, anthropic contamination by droplets and biological fluids is widespread in spaces open to the public and can be traced by RT-PCR. Monitoring fomites can support evaluation of indirect transmission risks for Coronavirus or other flu-like viruses in the environment.

57

58 **Importance**

59 Several studies searched for SARS-CoV-2 in the environment because saliva and nasopharyngeal
60 droplets can land on objects and surfaces creating fomites. However, the ideal indicator would be
61 the detection of the biofluid. This approach was not yet considered, but follows a traditional
62 principle in hygiene, using indicators rather than pathogens. We searched for viral RNA but also
63 for droplets on surfaces at risk. For the first time, we propose to monitor droplets thorugh their
64 microbiota, by RT-PCR or NGS.
65 Even if performed during the pandemic, SARS-CoV-2 wasnôt largely spread on surfaces, unless
66 in proximity of an infectious patient. However, anthropic contamination was frequently at high
67 level, suggesting a putative marker for indirect transmission and risk assessment. Moreover, all
68 SARS-CoV-2- contaminated surfaces showed the dropletsô microbiota.
69 Fomites detection may have an impact on public health, supporting prevention of indirect
70 transmission also for other communicable diseases such as Flu and Flu-like infections.

71

72

73

74

75

76 **GRAPHICAL ABSTRACT**

77

78

79

80

81

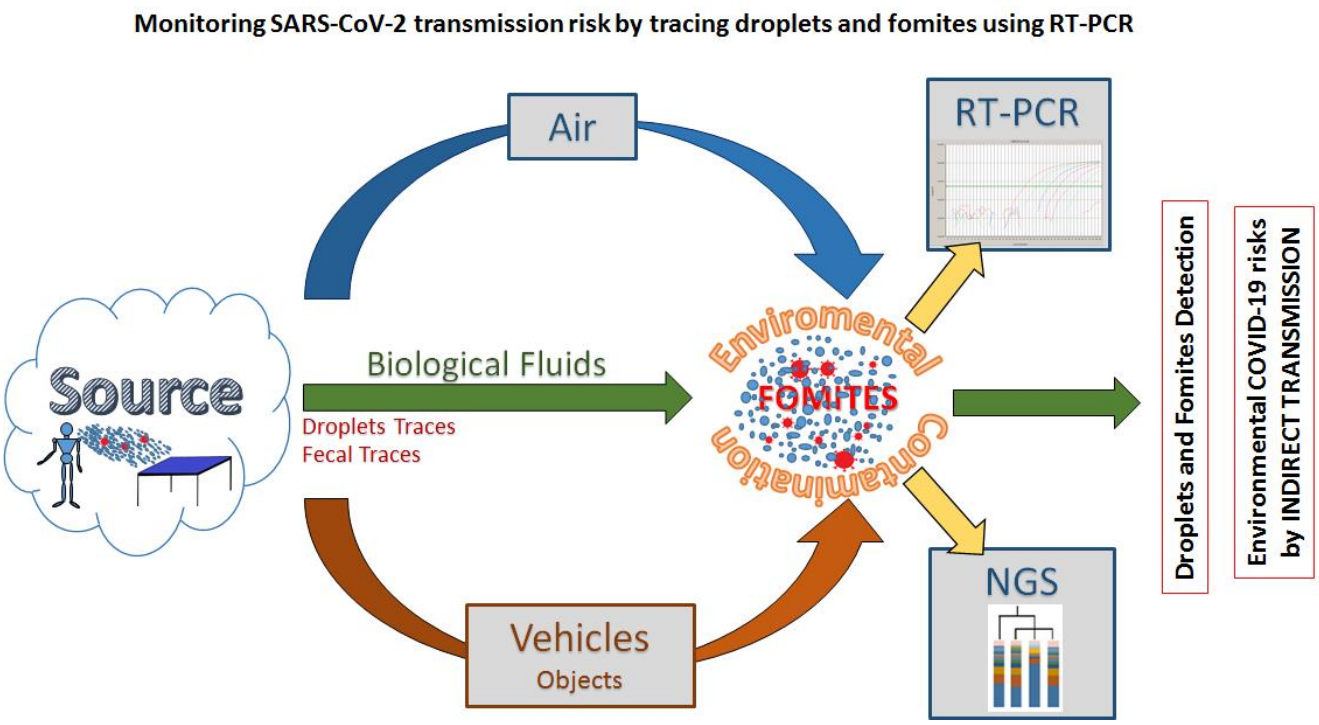

82

1 Introduction

The ongoing pandemic of coronavirus disease 2019 (COVID-19) is thought to have spread mainly through a direct route of transmission: by person to person close contact and inhalation of virus-laden liquid droplets (WHO, 2020; Stadnytskyi et al., 2020; Somsen et al., 2020; Liu et al., 2020; NCIRD, 2020; Asadi et al, 2020). However, it is also recognised that Severe Acute Respiratory Syndrome Coronavirus 2 (SARS-CoV-2) can follow an indirect route of transmission through environmental contamination of objects and surfaces, being carried by biological fluids such as saliva, nose secretions, and feces, in which viral RNA was consistently detected (Van Doremalen, et al., 2020; Chia et al., 2020; Guo, et al., 2020; Cheng et al., 2020; Ong et al., 2020; Lv et al., 2020; Razzini et al., 2020; Li et al., 2020; Chen et al., 2020; Foladori et al., 2020). Respiratory droplets (aerodynamic diameter ranging between >5 and 10 µm) and droplet nuclei or aerosols (Ò 5 µm) from a patient or an asymptomatic subject can reach directly the mouth, nose or eyes of a susceptible person, but can also land in the surroundings, creating contaminated surfaces, namely fomites (WHO, 2014; Wei et al., 2020; Otter et al., 2016; Al Huraimel et al., 2020). The risk of an indirect transmission through contaminated surfaces is related to the capability of the coronavirus to survive on different matrices under different conditions, persisting from hours to days, especially in indoor environments (Eslami and Jalili. 2020; Kampf et al., 2020; Hung et al., 2020). The question of evaluating the level of environmental contamination is important not only during outbreaks and the epidemic peak, but also during the transition phases, when asymptomatic infected carriers may release the virus in the environment by talking, coughing, sneezing, touching objects and consequently spreading contaminated biofluids (including saliva and nose secretions, faecal traces or droplets) (Kampf et al., 2020; Hung et al., 2020; Wu et al., 2020). This issue has already been considered in higher-risk environments such as hospitals and public areas, where

SARS-CoV-2 was clearly detected in several studies, even when surveillance and sanitation were accurately performed (Wu et al., 2020; Wang et al. 2020).

Finally, when approaching the question of the presence of SARS-CoV-2 in the environment, we need to consider that the pathogen is conveyed by biological fluids. Therefore, the possibility of detecting fomites and biological fluids in the environment becomes both a potential marker of hygiene levels, and also a candidate indicator for indirect COVID-19 transmission risks. Starting from this working hypothesis, we surveyed hospitals and public buildings not simply for the presence of SARS-CoV-2, but also for the presence of droplets, fomites and anthropic contaminations, by searching traces of the microbiota signature of their own biological fluids of origin. To address this issue, a dedicated set of primers and probes was combined to detect different biological fluids based on multiplex reactions in real-time PCR (RT-PCR), following a strategy initially developed for forensic studies and hospital hygiene (Giampaoli et al., 2012; Giampaoli et al., 2014; Valeriani et al., 2016; Valeriani et al., 2018a; Yao et al., 2020). Thus, a same general approach based on RT-PCR was considered to test both the viral RNA by standard procedures and the DNA from fomites by microbiota signature. The general principle is based on the amplification of genes from at least one representative bacterial component of the biological fluid, e.g. amplifying bacterial genes from *E. salivarius* and *S. mutans* for targeting saliva, or *Corynebacterium* for nose secretions, or *E. faecalis* and *Bacteroides* for evaluating the presence of faecal traces, as previously shown (Esberg et al., 2020; Liu et al., 2020; Charles et al., 2019; Proctor et al., 2019; Lloyd-Price, J et al., 2016). This approach can be confirmed by next generation sequencing (NGS), analysing the whole microflora DNA (mfDNA) as sampled with environmental swabs on indoor and outdoor surfaces (Slatko et al., 2018; Valeriani et al., 2018b; Valeriani et al., 2018c; Valeriani et al., 2019; Mucci et al., 2020).

The overall aim of this study was to search for both SARS-CoV-2 and fomites in hospitals and public buildings, to evaluate the possibility of monitoring by RT-PCR fomites and biofluid contamination, as a novel indicator of hygiene as well as a candidate marker for indirect transmission risks for COVID-19.

2. Materials and Methods

2.1. Sampling and experimental design

Surfaces at risk for the presence of biological fluids and the transmission of COVID-19 were sampled from different settings, both in indoor and outdoor areas. Environmental samples (n=94) were collected after the epidemic peak in Italy (May-June 2020). We sampled indoor surfaces from three COVID-reference hospitals in three Italian regions (Parma, Emilia-Romagna; Sassari, Sardinia; Rome, Lazio); buildings open to public use (1 office, 1 fast food, 1 church); outdoor areas; and used handkerchiefs with nasopharyngeal secretions. Samples were tested for SARS-CoV-2 RNA, whereas anthropic contamination was assessed searching for biological fluids of nose, mouth, gut through their microbiota traces by RT-PCR and/or NGS (Table 1).

2.2. Sampling collection

Surface sampling was carried out after their use and prolonged exposure to human presence (>4h). Following standard protocols, FLOGSwabs and CITOSSWAB were used and soaked into a buffer solution in a volume of 400 µl of UTM-RM transport medium (Copan Diagnostics Inc., Murrieta, CA, USA). The nasopharyngeal secretions were collected on handkerchiefs with swabs (4N6FLOQSwabs, Copan Diagnostics Inc., Murrieta, CA, USA). All specimens were refrigerated at 4°C if testing could postpone in the following days.

153

154 **2.3. SARS-CoV-2 detection**

155 All samples in UTM were heat inactivated at 56°C for 5 minutes to reduce the risk of accidental
156 transmission of SARS-CoV-2 to laboratory personnel. Nucleic acids were purified and extracted
157 using the eMag automated nucleic acid sample extraction system (bioMérieux, Marcy lõEtoile,
158 France). Briefly, total nucleic acids were extracted from UTM using an input sample volume of
159 200 µl into 2,000 µl of easyMag lysis buffer using B protocol to a final eluted volume of purified
160 nucleic acids of 50 µl. TaqPath 1-step reverse transcriptase quantitative PCR (RT-qPCR) master
161 mix (Life Technologies, Frederick, MD) and the 2019- nCoV CDC EUA kit (Integrated DNA
162 Technologies, Coralville, IA) were used for target detection (*CDC, 2020*). Molecular detection of
163 SARS-CoV-2 RNA was carried out by rRT-PCR, using primers and probes related to the E gene,
164 with a detection limit of 5.2 copies of RNA/reaction (Corman V. 2019). Samples were analyzed
165 in Sassari and Parma with the Allplex 2019-nCoV assay (Seegene, Seoul, South Korea) and in
166 Rome with the Detection Kit for 2019 Novel Coronavirus (2019-nCoV) RNA (PCR-Fluorescence
167 Probing) (Daan Gene Co., Ltd of Sun Yat-University, Guangzhou, Guandong, China) for the
168 confirmation of the results. The Allplex 2019-nCoV assay was designed for amplifying three viral
169 targets: the E gene (subgenus Sarbecovirus), the N, and the RdRP genes (Farfour, 2020). The
170 Detection Kit for 2019 Novel Coronavirus (2019-nCoV) RNA (PCR-Fluorescence Probing) is a
171 CE-marked RT-PCR assay which simultaneously detects the viral nucleocapsid N and Orf1ab
172 genes. Afterward, 5 µl of eluted RNA samples in a total volume of 25 µl were RT-PCR amplified
173 on Biorad CFX96 real-time system. In each round of extraction and amplification, positive and
174 negative control samples (supplied by the manufacturer) were included. The interpretation criteria
175 were the following: 1) positive signals detected in ORF1ab and N genes with a cycle threshold
176 (Ct) values Ò40 were considered positive for SARS-CoV-2 RNA; 2) positive signals in only one

177 gene (N or Orf1ab) with a Ct values Ò40 were considered inconclusive; and 3) no fluorescent
178 signals or over the 40th Ct in ORF1ab and N genes were considered not specific and reported as
179 negative for SARS-CoV-2 RNA. The declared LoD is 500 RNA copies/ml.
180
181 **2.4. DNA extraction**
182 An aliquot of COPAN UTM-RM transport medium (about 300 ε L) was centrifugated at 16000 g
183 for 10 minutes and the pellet was manually disaggregated with a pestle after adding glass beads
184 (Sigma-Aldrich, St Louis, MO) and lysed in 200 ε L lysozyme solution, RNase A treated, and
185 proteinase K digested according to the GenElute Bacterial Genomic DNA Kit (Sigma Aldrich, St
186 Louis, USA). Finally, DNA elution was performed in 60 ε L elution solution (10 mM
187 tris(hydroxymethyl)aminomethane-hydrochloride and 0.5mM ethylene diamine tetra acetic acid,
188 pH 9.0). For pharyngeal biofluids and fomites samples, each swab was inserted into the
189 semipermeable NAO Baskets and broken inside at the breakpoint. Approximately 200 ε L
190 lysozyme solution (20mg/mL Lisozima, 20 mM tris[hydroxymethyl]aminomethanehydrochloride
191 at pH 8, 2mM ethylenediaminetetraacetic acid, and 1.2%TritonX-100; Sigma Aldrich, St Louis,
192 USA) were added into the NAO Baskets and incubated a 37°C for 30 minutes. Then, 20 ε L
193 proteinase K and 400 ε L buffer AL were added and the sample was centrifuged at 10,000 × g for
194 1 minute, allowing the elution of the digestion solution. After incubation at 56°C for 10 minutes
195 and addition of 400 ε L ethanol, the washing step and DNA puriý cation were performed in
196 accordance with the manufacturerôs instructions. DNA elution was completed in 60 ε L elution
197 solution (10 mM tris[hydroxymethyl]aminomethane-hydrochloride and 0.5 mM
198 ethylenediaminetetraacetic acid at pH 9.0), as previously described (Cianfanelli et al., 2017;
199 Valeriani et al., 2017; Valeriani et al., 2018c;).
200

201 **2.5. Analysis of mfDNA by multiplex real-time PCR and data interpretation**

202 Ampliýcations were combined in 4 multiplex reactions: mix Skin, for the identiýcation of
203 *Staphylococcus aureus* and *Staphylococcus epidermidis*; mix Nasopharynx for *Propionibacterium*
204 *spp.* and *Corynebacterium spp.*; Mix oralpharinx for *Streptococcus salivarius* and *Streptococcus*
205 *mutans*; mix feces for *Enterococcus spp* and *Bacteroides vulgatus* (probes were labeled
206 FAM/VIC/HEX, with the BHQ-1quencher). Primers for different bacterial indicators and
207 optimized reaction conditions were already established, as previously described (Elshi et al., 2000;
208 Giampaoli et al., 2012; Chung et al., 2016; Valeriani et al. 2018a; Byrd et al., 2018; Liu, Q. 2020).
209 Briefly, amplifications were performed in a volume of 25 εL, of which 12.5 εL JumpStart Taq
210 ReadyMix for Quantitative PCR (Sigma Aldrich, St. Louis, MO), containing 900nM forward and
211 reverse primers, and 250 nM of each probe. For each mix, samples were tested in triplicate. The
212 ampliýcations were performed using Bio-RadCFX96(Bio-Rad,Hercules, CA) programmed for 10
213 minutes at 95°C and 40 cycles of 15 seconds at 95°C and 1 minute at 60°C. For each sample 11
214 εL template reaction was ampliýed. The PCR output was expressed as cycle threshold (CT).
215 Positive samples were those where Ó1 positive indicator (CT Ò35) was found in at least 2 mixes.
216 Conversely, a microbial indicator was considered negative when over the CT Ó39 threshold.

217

218 **2.5. 16S rDNA Amplicon sequencing analysis**

219 Libraries for NGS were prepared according to the 16S Metagenomic Sequencing Library
220 Preparation Guide (part# 15044223 rev A; Illumina, San Diego, CA, USA). The PCR amplicons
221 were obtained using Ba27F and Ba338R primers containing overhang adapters, as previously
222 described (40, 41). Tagged PCR products were generated using primer pairs with unique barcodes
223 through two-step PCR. In this strategy, target primers containing overhang adapters were used in
224 the first PCR reaction to amplify the target gene, that product was then used in the second PCR

using primers-containing barcodes. Each amplification reaction had a total volume of 25 εL, containing 12.5 εL of KAPA HiFi Hot Start Ready Mix (Roche, Pleasanton, CA, USA), 5 εL of each primer (1 εM), and 2 εL of template DNA. Reactions were carried out on a Techne®TC-PLUS thermocycler (VWR International, LLC, Radnor, PA, USA). Following amplification, 5 εL of PCR product from each reaction was used for agarose gel (1%) electrophoresis to confirm amplification. The final concentration of cleaned DNA amplicon was determined using the Qubit PicoGreen dsDNA BR assay kit (Invitrogen, Grand Island, NY, USA) and validated on a Bioanalyzer DNA 1000 chip (Agilent, Santa Clara, CA, USA). Libraries were prepared using the MiSeq Reagent Kit Preparation Guide (Illumina, San Diego, CA, USA). Raw sequence data was processed using an in-house pipeline that was built on the Galaxy platform and incorporated various software tools to evaluate the quality of the raw sequence data (FASTA/Q Information tools, Mothur). All datasets were rigorously screened to remove low-quality reads (short reads >200 nt, zero-ambiguous sequences). Demultiplexing was performed to remove PhiX sequences and sort sequences; moreover, to minimize sequencing errors and ensure sequence quality, the reads were trimmed based on the sequence quality score using Btrim (an average quality score of 30 from the ends, and remove reads that are less any 200 bp after end-trimming) (Kong, 2011). OTUs (operational taxonomic units) were clustered at a 97% similarity level, and final OTUs were generated based on the clustering results, and taxonomic annotations of individual OTUs were based on representative sequences using RDPôs 16S Classifier 2.5. Observed OTUs were defined as observed species. A level of 97% sequence identity is often chosen as representative of a species and 95% for a genus. The sequence reads were analyzed, also, in the cloud environment BaseSpace through the 16S Metagenomics app (version 1.0.1; Illumina®): the taxonomic database used was the Illumina-curated version (May 2013 release of the Greengenes Consortium Database) (Wang et al., 2013).

2.6. Statistical Analysis

Relative abundances of community members were determined with rarefied data and summarized at each taxonomic level. The proportion of the microbiome at each taxonomic rank, such as phylum, order, class, family, and genus, was determined using the RDP classifier and the Greengenes Database. Alpha and beta diversity were calculated using EstimateS software at a level of 97% sequence similarity. Regarding alpha diversity, the Shannon index and equitability index at the species level were computed (Colwell et al., 2012; Magurran, 2016). Principal component analysis (PCA) was performed using the METAGENassist platform and and R (version 3.1.3, www.R-project.org) with packages ñggplot2ò, ñapeò, ñpsychò and ñveganò (Arndt et al., 2012). Multivariate analysis, the PCA, and partial least square-discriminant analysis (PLS-DA) were performed in order to investigate the dissimilarity between groups. Feature selection was performed using PLS-DA and 10-fold cross validation to tune algorithm parameters and to check model validity. Dendrogram and clustering analysis were based on the Euclidean distance and Wardôs method.

3. Results and discussion

3.1 Detection of fomites by RT-PCR

Anthropic contamination by droplets and biofluids was detected on different environmental surfaces by RT-PCR (Table 2). The presence of fomites appeared largely diffused in indoor and outdoor areas exposed to human crowding or frequently touched with hands. Floors and walls were less contaminated than handles or buttons. Droplets DNA traces were detected in most of surfaces and almost 10% of sampled points displayed a multiple contamination from different biological

fluids. Correlation between selected bacterial species and biological fluids in droplets and fomites was confirmed (p-value <0.01) (Table 3), supporting the effectiveness of the approach. The combined action of different markers is synergic (Figure 1), allowing a reliable identification of droplets and fomites. Indoor and outdoor samples showed the presence of traces from one or more human biofluids, although with different intensity. Being a quantitative approach, indeed, RT-PCR can provide not only a qualitative output for the presence of droplets traces, but also an indication on the contamination level, allowing to set different thresholds or report CT data in the form of genomic units. However, the definition of a more precise quantitative interpretation of the multiplex amplification output would require a larger exploitation of the method, based on different environments, monitoring purposes or expected hygiene levels. The procedure to extract nucleic acid and detect anthropic contamination from environmental swabs could be automatize, likewise already done for testing SARS-CoV-2 from human swabs; therefore, detection of fomites by RT-PCR seems a feasible and promising approach even on a larger scale.

3.2 SARS-CoV-2 in hospitals and public places

SARS-CoV-2 was not detected in most of the sampling points, both indoor and outdoor. It was not found in all 15 sampling points within the air system of a COVID-19 hospital. SARS-CoV-2 RNA was detected only in one room where an infected patient was hospitalized and only in those samples collected near to the patient (one on the bed rail and one on the surface of the call button). The stethoscope used on the patient was positive, too. The low frequency (<4%) of positive samples in comparison with other studies (20-30%) can be associated to differences in the sampling strategy or to a lower sensitivity of the method (Liu, Y., 2020); moreover, it depends on the epidemiological scenario when the study was carried out, at time when reopening of activities

was carefully surveilled and preventive measures were strictly enforced (Pasquarella, 2020; Di Maria, 2020; Veronesi, 2020; Van Doremalen, et al., 2020; Chia et al., 2020; Guo, et al., 2020; Cheng et al., 2020; Ong et al., 2020; Lv et al., 2020; Razzini et al., 2020; Li et al., 2020; Chen et al., 2020; Foladori et al., 2020; Wei et al., 2020). From our findings, it seems that the environmental spread of SARS-CoV-2 was not widely diffused, with the only exception of the surfaces near a hospitalized infected patient.

3.3 NGS analysis.

The microbial signature obtained by RT-PCR was confirmed by NGS and all selected bacterial indicators were also included within the microbiota identified by high-throughput sequencing and bioinformatic analysis. RT-PCR and NGS characterized environmental samples based on their contamination patterns: by CT analysis on selected marker genes or by reads count on all 16S amplicon sequences, respectively (Figures 2 and 3). DNA test can be easily performed within one day on any real time apparatus, whereas NGS within one week adapting the laboratory protocol to the high throughput sequencer and accomplishing the required bioinformatic evaluation on the obtained data. However, NGS provides the 16S rDNA sequences of all the bacterial species in the sample, so that any anthropic contamination can represent just only a minority of the resident or acquired microflora on a surface. Therefore, each selected indicator specifically amplified by RT-PCR was observed by NGS, but only as a subcomponent between others (about 200-1000 species for each sample), including the unknown species (about 5-10%). Mean values ranged from 0.24% (*Bacteroides*) to 5.78% (*Corynebacterium*). For example, *Corynebacterium* showed lower values (<1%) in environmental samples exposed to multiple sources of microbial pollutions, whereas the highest values (35-80%) were observe in environmental swabs collected from human

nasopharyngeal secretions, further confirming the specific role of that marker within the microbial signature of the biological fluid. Nevertheless, both methods provided similar dendrograms. The correspondence between RT-PCR and NGS was reliable: two independent SARS-CoV-2 positive samples (YH1_01 and YH1_05) collected from same patient surroundings closely gathered, whereas the sample collected from the stethoscope used on the same patient (YH1_12) segregated at a different distance, in both dendrograms. Indeed, the anthropic contaminations present on the right side of the bed (YH1_01) and on the call bottom (YH1_05) showed a similar biodiversity pattern (as also shown by the Shannon index 2.602 and 2.893, respectively), characterized by the presence of traces from different biofluids, suggesting a possible contamination through the patient right hand. Conversely, sample YH1_12 displayed microbiota traces mainly restricted to nasopharyngeal secretions and with a different biodiversity pattern (Shannon index 2.161), suggesting a possible contact of the stethoscope on the patient chest (probably contaminated after a sneeze without keeping the mask). Eventually, NGS provided a more comprehensive overview of all the environmental bacteria present on the sampled surfaces, confirming also those coming from the microbiota of human biological fluids.

3.4 Fomites and environmental microflora

Environmental contamination through droplets or biofluids that can convey SARS-CoV-2 represents an additional component of the complex microflora detectable on a surface. Indeed, the identification of fomites by RT-PCR analysis of selected indicators emphasizes a very specific - and often minority- component of the resident or ectopic microflora. The analysis of the dataset by NGS showed not only the wide presence of fomites on several surfaces exposed to anthropic contamination, but also the inhabiting microorganisms or those from other environmental sources.

Samples collected from indoor and outdoor surfaces gathered independently from human biofluids (Figure 5). Within the outdoor group, those with a higher anthropic contamination overlapped with indoor samples, far from those where the environmental component was overwhelming. Interestingly, only an outdoor sample segregated outside -and in between- of both groups: the external handle of the entrance of a public building (Z_04), characterized by multiple contaminations of anthropic origin overlaying the outside microflora. Other indoor samples grouped together. These findings support the utility of microbiota data for tracing fomites in environmental samples and can sustain risk assessment for an indirect transmission of COVID-19. Nevertheless, the detection of traces of biological fluids in several environmental surfaces did not predict the presence of SARS-CoV-2, unless in virus positive points, even if sampling occurred during the pandemic period and in hospitals where COVID-19 patients were treated. Therefore, if fomites represent a risk themselves, the possibility for a contagion relays on the presence of the specific pathogen and its viability, satisfying the principles from the ancient Kochôs postulates (Segre, 2013). Moreover, even if detectable through its RNA, the environmental survival of SARS-CoV-2 depends on different indoor and outdoor factors, including sanitation, time from the release of the biological fluid, exposure to agents such as humidity, temperature, air circulation and sunlight (Aboubakr, 2020; Morawska, 2020; Yolitz, 2020; Ratnesar-Shumate, 2020; Biryukov, 2020). Therefore, viral infectivity can vary significantly between different environments and detection of fomites should be considered more as a putative indicator of transmission risk levels, than a danger itself. Monitoring droplets and biofluids by RT-PCR can help to prevent SARS-CoV-2 transmission by improving environmental surveillance and enforcing hygiene and sanitization procedures.

3.5 Critical issues and limits of the study

Even if several surfaces at risk of indirect transmission were evaluated, the study aim was not the quantification of the infectious risk. Comparisons between sampling points or buildings cannot be performed, not only for the sample size but also for the random collection from areas with a different incidence of disease. Indeed, different Italian regions were selected to avoid geographical bias, but different epidemiological burdens can affect the generalizability of the results. Therefore, we have simply reported an environmental scenario, suggesting a possible strategy to assess contaminations at risk for indirect transmission of COVID-19. Interestingly, SARS-CoV-2 positive samples were collected only in Emilia-Romagna, a region with the highest number of cases in Italy (Veronesi et al., 2020). Thus, this is not an epidemiological study aimed at comparing geographical areas or quantify a risk for a specific environment or sampled surface. Nevertheless, observed data clearly identify surfaces at risk and confirm the fundamental role played by hands. Regarding the chosen approach, RT-PCR is faster than NGS (3-5 hours vs 5-10 days), but still is not instantaneous, as other strategies aimed to detect contaminations on surfaces or medical devices (Valeriani, 2018 a; Lee, 2020).Tracing droplets and identifying biological fluids by RT-PCR or NGS is specific respect to other methods based on finding organic matter without a recognition of their origin, e.g. from human secretions rather than human cells, plant, animal or bacterial debris. Therefore, detection of droplets by RT-PCR is not a generic marker of hygiene but can find specific application also in assessing environmental risks for other communicable diseases following an indirect rout of transmission, such as flu-like infections (Otter et al., 2016; Petersen, 2020; Wei et al., 2020).

Another limitation concerns the set of experimental conditions for RT-PCR and NGS. Primers and probes for selected bacterial genes from selected bacterial markers where chosen because of their

387 feasibility and effectiveness, but we did not made comparisons with different sequences, indicators
388 or reaction conditions for RT-PCR. The same concern can be raised for the NGS approach, which
389 was adopted for the analysis of 16S rDNA amplicon sequencing, following standard protocols. A
390 whole genome analysis would have been more informative. However, it would have also been
391 more expensive for materials and bioinformatic analysis, being less appropriate for public health
392 surveys on a larger scale. Finally, we used arbitrary thresholds to quantify droplets contamination
393 based on CT values, proposing the highest sensibility for droplets detection. A lower threshold
394 would have provided more specific data, or it could have been adapted to the different kind of
395 transmission risks or expected hygiene levels in the different environments.

396

397

398 **Conclusions**

399 Environmental monitoring of fomites with a potential role in COVID-19 transmission, can be
400 performed by RT-PCR. The general principle is based on the identification of anthropic
401 contaminations by detecting their microbiota component.

402 Droplets and biological fluids were observed in most of the indoor places exposed to human
403 presence, and on those surfaces frequently touched by hands. SARS-CoV-2 was not detectable
404 diffusely in the environment, except in the proximity of an infected patient and in consistent
405 association with fomites. The whole of the results supports the key role of handwashing and
406 environmental sanitation in reducing risks related to indirect transmission of COVID-19 in
407 hospitals or public areas, both indoor and outdoor. It also highlights the role of education and
408 awareness in protecting the health of all.

409 In addition to searching for SARS-CoV-2 in the environment, the possibility to detect fomites by
410 RT-PCR may provide a novel indicator for monitoring indirect transmission risks of COVID-19
411 as well as other communicable diseases transmitted through droplets, such as flu or flu-like
412 infections.

413

414

Acknowledgments

The authors would like to thank dr. Elena Scaramucci, Tiziana Zilli and Pietro Robert for supporting bibliography search and management; Alessandro Stabile for assuring laboratory safety and acceptance of reagents during summertime; the Copan Italia S.p.A. Brescia Italy for providing eNATand UTM collection kits. This study was partially supported by University of Foro Italico Project (CDR2.TER012013) assigned to V.R.S.

References

Aboubakr, H.A., Sharafeldin, T.A., Goya, S.M. 2020. Stability of SARS-CoV-2 and other coronaviruses in the environment and on common touch surfaces and the influence of climatic conditions: A review. Transbound Emerg Dis. 00:1-17 https://doi.org/10.1111/tbed.13707

Al Huraimel, K., Alhosani, M., Kunhabdulla, S., Stietiya, M. H. 2020. SARS-CoV-2 in the environment: Modes of transmission, early detection and potential role of pollutions. The Science of the total environment. 744, 140946. Advance online publication. https://doi.org/10.1016/j.scitotenv.2020.140946.

Arndt, D., Xia, J., Liu, Y., Zhou, Y., Guo, A.C., Cruz, J.A., Sinelnikov, I., Budwill, K., Nesbø, C.L., Wishart, D.S. 2012. METAGENassist: a comprehensive web server for comparative metagenomics. Nucleic Acids Res. 40, 88-95. https://doi.org/10.1093/nar/gks497

Asadi S, Wexler AS, Cappa CD, Barreda S, Bouvier NM, Ristenpart WD. 2020. Effect of voicing and articulation manner on aerosol particle emission during human speech. PLoS One;15(1): e0227699. doi: 10.1371/journal.pone.0227699. eCollection 2020.

Biryukov, J., Boydston, J.A., Dunning, R.A., Yeager, J.J, Wood, S., Reese, A.L., Ferris, Q., Miller, D., Weaver, W., Zeitouni, N.E., Phillips,A., Freeburger, D., Hooper, I., Ratnesar-Shumate. S., Yolitz, J., Krause, M., Williams, G., Dawson, D.G., Herzog, A., Dabisch, P., Wahl, V., Hevey, M.C., Altamura, L.A. 2020. Increasing Temperature and Relative Humidity Accelerates Inactivation of SARS-CoV-2 on Surfaces. mSphere. 5(4):e00441-20. Published 2020 Jul 1. https://doi.org/10.1128/mSphere.00441-20

Byrd, A.L., Belkaid,Y., Segre, J.A. 2018. The human skin microbiome. Nature Reviews Microbiology. 16,143ï 155. https://doi.org/10.1038/nrmicro.2017.157.

CDC, Centers for Disease Control and Prevention. 2020. CDC 2019-novel coronavirus (2019-nCoV) real-time RT-PCR diagnostic panel services. Centers for Disease Control and Prevention, Atlanta, GA. https://www.fda.gov/media/134922/download (access 10 August 2020).

Charles, D. D., Fisher, J. R., Hoskinson, S. M., Medina-Colorado, A. A., Shen, Y. C., Chaaban, M. R., Widen, S. G., Eaves-Pyles, T. D., Maxwell, C. A., Miller, A. L., Popov, V. L., & Pyles, R. B. 2019. Development of a Novel ex vivo Nasal Epithelial Cell Model Supporting Colonization with Human Nasal Microbiota. Frontiers in cellular and infection microbiology. 9, 165. https://doi.org/10.3389/fcimb.2019.00165.

Chen, Y., Chen, L., Deng, Q., Zhang, G., Wu, K., Ni, L., Yang, Y., Liu, B., Wang, W., Wei, C., Yang, J., Ye, G., & Cheng, Z. 2020. The presence of SARS-CoV-2 RNA in the feces of COVID-19 patients. Journal of medical virology. 92(7), 833ï 840. https://doi.org/10.1002/jmv.25825.

Cheng, V.C.C., Wong, S.C., Chan, V.W.M., So, S.Y.C., Chen, J.H.K., Yip, C.C.Y., Chan, K.H., Chu, H., Chung, T.W.H., Sridhar, S., To, K.K.W., Chan, J.F.W., Hung, I.F.N., Ho, P.L., Yuen, K.Y. Air and environmental sampling for SARS-CoV-2 around hospitalized patients with coronavirus disease 2019 (COVID-19). Infect Control Hosp Epidemiol. 1-32. https://doi.org/10.1017/ice.2020.2822020.

Chia, P.Y., Coleman, K.K., Tan, Y.K., Ong, S.W.X., Gum, M., Lau, S.K., Lim, X.F., Lim, A.S., Sutjipto, S., Lee, P.H., Son, T.T., Young, B.E., Milton, D.K., Gray, G.C., Schuster, S., Barkham, T., De, P.P., Vasoo S., Chan, M., Ang, B.S.P., Tan, B.H., Leo,Y.S., Ng, O.T., Wong, M.S.Y., Marimuthu, K., and for the Singapore 2019 Novel Coronavirus Outbreak Research Team. 2020. Detection of air and surface contamination by SARS-CoV-2 in hospital rooms of infected patients. Nat Comm. 11(1), 1-7. https://doi.org/10.1038/s41467-020-16670-2.

Colwell, R.K., Chao, A., Gotelli, N.J., Lin, S.Y., Mao, C.X., Chazdon, R.L., Longino, J.T. 2012. Models and estimators linking individual-based and sample-based rarefaction, extrapolation, and comparison of assemblages. Journal of Plant Ecology. 5, 3-21. https://doi.org/10.1093/jpe/rtr044.

Corman VM, Landt O, Kaiser M, Molenkamp R, Meijer A, Chu DK, Bleicker T, Brünink S, Schneider J, Schmidt ML, Mulders DG, Haagmans BL, van der Veer B, van den Brink S, Wijsman L, Goderski G, Romette JL, Ellis J, Zambon M, Peiris M, Goossens H, Reusken C,

Koopmans MP, Drosten C. 2020. Detection of 2019 novel coronavirus (2019-nCoV) by real-time RT-PCR. Euro surveillance: European communicable disease bulletin, 25(3), 2000045. https://doi.org/10.2807/1560-7917.ES.2020.25.3.2000045.

Di Maria, F., Beccaloni, E., Bonadonna, L., Cini, C., Confalonieri, E., La Rosa, G., Milana, M. R., Testai, E., Scaini, F. 2020. Minimization of spreading of SARS-CoV-2 via household waste produced by subjects affected by COVID-19 or in quarantine. The Science of the total environment, 743, 140803. Advance online publication. https://doi.org/10.1016/j.scitotenv.2020.140803.

Esberg, A., Haworth, S., Kuja-Halkola, R., Magnusson, P., & Johansson, I. 2020. Heritability of Oral Microbiota and Immune Responses to Oral Bacteria. Microorganisms. 8(8), E1126. https://doi.org/10.3390/microorganisms8081126.

Eslami, H., Jalili, M. 2020. The role of environmental factors to transmission of SARS-CoV-2 (COVID-19). AMB Express. 10(1), 92. https://doi.org/10.1186/s13568-020-01028-0

Farfour, E., Lesprit, P., Visseaux, B., Pascreau, T., Jolly, E., Houhou, N., Mazaux, L., Asso-Bonnet, M., Vasse, M., & SARS-CoV-2 Foch Hospital study group. 2020. The Allplex 2019-nCoV (Seegene) assay: which performances are for SARS-CoV-2 infection diagnosis? European journal of clinical microbiology & infectious diseases: official publication of the European Society of Clinical Microbiology, 10.1007/s10096-020-03930-8. Advance online publication. https://doi.org/10.1007/s10096-020-03930-8.

Foladori, P., Cutrupi, F., Segata, N., Manara, S., Pinto, F., Malpei, F., Bruni, L., La Rosa, G. 2020. SARS-CoV-2 from faeces to wastewater treatment: What do we know? A review. The Science of the total environment. 743, 140444. Advance online publication. https://doi.org/10.1016/j.scitotenv.2020.140444.

Giampaoli, S., Alessandrini, F., Berti, A., Ripani, L., Choi, A., Crab, R., De Vittori, E., Egyed, B., Haas, C., Lee, H. Y., Korabecná, M., Noel, F., Podini, D., Tagliabracci, A., Valentini, A., & Romano Spica, V. 2014. Forensic interlaboratory evaluation of the ForFLUID kit for vaginal fluids identification. Journal of forensic and legal medicine. 21, 60ï 63. https://doi.org/10.1016/j.jflm.2013.10.016.

Giampaoli, S., Berti, A., Valeriani, F., Gianfranceschi, G., Piccolella, A., Buggiotti, L., Rapone, C., Valentini, A., Ripani, L., & Romano Spica, V. 2012. Molecular identification of vaginal fluid

by microbial signature. Forensic science international. Genetics. 6(5), 559ï 564. https://doi.org/10.1016/j.fsigen.2012.01.005.

Guo, Z.D., Wang, Z.Y., Zhang, S.F., Li, X., Li, L., Li, C., Cui, Y., Fu, R.B., Dong, Y.Z., Chi, X.Y., Zhang, M.Y., Liu, K., Cao, C., Liu, B., Zhang, K., Gao, Y.W., Lu, B., Chen, W. 2020. Aerosol and Surface Distribution of Severe Acute Respiratory Syndrome Coronavirus 2 in Hospital Wards, Wuhan, China, 2020. Emerg Infect Dis. 26(7). doi.org/10.3201/eid2607.200885

Hung IF, Cheng VC, Li X, Tam AR, Hung DL, Chiu KH, Yip CC, Cai JP, Ho DT, Wong SC, Leung SS, Chu MY, Tang MO, Chen JH, Poon RW, Fung AY, Zhang RR, Yan EY, Chen LL, Choi CY, Leung KH, Chung TW, Lam SH, Lam TP, Chan JF, Chan KH, Wu TC, Ho PL, Chan JW, Lau CS, To KK, Yuen KY. 2020. SARS-CoV-2 shedding and seroconversion among passengers quarantined after disembarking a cruise ship: a case series. The Lancet. Infectious diseases, S1473-3099(20)30364-9. Advance online publication. https://doi.org/10.1016/S1473-3099(20)30364-9.

Kampf, G., Todt, D., Pfaender, S., Steinmann, E. 2020. Persistence of coronaviruses on inanimate surfaces and their inactivation with biocidal agents. The Journal of hospital infection. 104(3), 246ï 251. https://doi.org/10.1016/j.jhin.2020.01.022.

Kong, Y. 2011. Btrim: a fast, lightweight adapter and quality trimming program for next-generation sequencing technologies. Genomics. 98(2), 152-153. https://doi.org/10.1016/j.ygeno.2011.05.009.

Lee, Y. M., Kim, Y. J., Kim, D. Y., Park, K. H., Lee, M.S. 2020. Monitoring environmental contamination caused by SARS-CoV-2 in a healthcare facility by using adenosine triphosphate testing. American journal of infection control, S0196-6553(20)30631-3. Advance online publication. https://doi.org/10.1016/j.ajic.2020.06.207.

Li, H.Y., Fan, Y.Z., Jiang, L., Wang, H.B. 2020. Aerosol and environmental surface monitoring for SARS-Cov-2 RNA in a designated hospital for severe COVID-19 patients. Epidemiology and Infection, 148, e154, 1-5. https://doi.org/10.1017/S0950268820001570.

Liu, Q., Liu, Q., Meng, H., Lv, H., Liu, Y., Liu, J., Wang, H., He, L., Qin, J., Wang, Y., Dai, Y., Otto, M., Li, M. 2020. Staphylococcus epidermidis Contributes to Healthy Maturation of the Nasal Microbiome by Stimulating Antimicrobial Peptide Production. Cell host & microbe. 27(1), 68ï 78.e5. https://doi.org/10.1016/j.chom.2019.11.003.

532 Liu, Y., Ning, Z., Chen, Y., Guo, M., Liu, Y., Gali, N. K., Sun, L., Duan, Y., Cai, J., Westerdahl,
533 D., Liu, X., Xu, K., Ho, K. F., Kan, H., Fu, Q., & Lan, K. 2020. Aerodynamic analysis of SARS-
534 CoV-2 in two Wuhan hospitals. Nature. 582(7813), 557-560. https://doi.org/10.1038/s41586-
535 020-2271-2273.

536 Lloyd-Price, J., Abu-Ali, G. & Huttenhower, C. The healthy human microbiome. 2016. Genome
537 Med 8, 51. https://doi.org/10.1186/s13073-016-0307-y.

538 Lv, J., Yang, J., Xue, J., Zhu, P., Liu, L., & Li, S. 2020. Detection of SARS-CoV-2 RNA residue
539 on object surfaces in nucleic acid testing laboratory using droplet digital PCR. The Science of the
540 total environment, 742, 140370. Advance online publication.
541 https://doi.org/10.1016/j.scitotenv.2020.140370.

542 Magurran, A.E. Measuring biological diversity. Wiley-Blackwell: Oxford, UK; 2016.

543 Morawska L, Tang JW, Bahnfleth W, Bluyssen PM, Boerstra A, Buonanno G, Cao J, Dancer S,
544 Floto A, Franchimon F, Haworth C, Hogeling J, Isaxon C, Jimenez JL, Kurnitski J, Li Y,
545 Loomans M, Marks G, Marr LC, Mazzarella L, Melikov AK, Miller S, Milton DK, Nazaroff W,
546 Nielsen PV, Noakes C, Peccia J, Querol X, Sekhar C, Seppänen O, Tanabe SI, Tellier R, Tham
547 KW, Wargocki P, Wierzbicka A, Yao M. 2020. How can airborne transmission of COVID-19
548 indoors be minimised? Environment International, 142, 105832.
549 https://doi.org/10.1016/j.envint.2020.105832

550 Mucci, N., Gianfranceschi, G., Cianfanelli, C., Santucci, S., Romano Spica, V., Valeriani, F.
551 2020. Can air microbiota be a novel marker for public health? A sampling model and preliminary
552 data from different environments. Aerobiologia, 36 (1): 71-75.

553 NCIRD, National Center for Immunization and Respiratory Diseases (NCIRD). 2020. How
554 COVID-19 spreads () https://www.cdc.gov/coronavirus/2019-ncov/about/transmission.html
555 (accessed 10 August 2020)

556 Ong, S.W.X., Tan, Y.K., Chia, P.Y., Lee, T.H., Ng, O.T., Wong, M.S.Y., Marimuthu, K. 2020.
557 Air, Surface Environmental, and Personal Protective Equipment Contamination by Severe Acute
558 Respiratory Syndrome Coronavirus 2 (SARS-CoV-2) From a Symptomatic Patient. JAMA.
559 323(16):1610-1612. https://doi.org/10.1001/jama.2020.3227.

560 Otter, J. A., Donskey, C., Yezli, S., Douthwaite, S., Goldenberg, S. D., Weber, D. J. 2016.
561 Transmission of SARS and MERS coronaviruses and influenza virus in healthcare settings: the

562 possible role of dry surface contamination. The Journal of hospital infection. 92(3), 235ï 250.
563 https://doi.org/10.1016/j.jhin.2015.08.027.

564 Pasquarella, C., Colucci, M. E., Bizzarro, A., Veronesi, L., Affanni, P., Meschi, T., Brianti, E.,
565 Vitali, P., & Albertini, R. 2020. Detection of SARS-CoV-2 on hospital surfaces. Acta bio-medica
566 Atenei Parmensis, 91(9-S), 76ï 78. https://doi.org/10.23750/abm.v91i9-S.10137.

567 Petersen, E., Koopmans,M., Go, U., Hamer, D.H., Petrosillo, N., Castelli, F., Storgaard, M., Al
568 Khalili, S., Simonsen,L. 2020. Comparing SARS-CoV-2 with SARS-CoV and influenza
569 pandemics Lancet Infect Dis. https://doi.org/10.1016/S1473-3099(20)30484-9.

570 Proctor, L., Lo Tempio, J., Marquitz, A., Daschner, P., Xi, D., Flores, R., Brown, L., Ranallo, R.,
571 Maruvada, P., Regan, K., Lunsford, R.D., Reddy, M., Caler, L. 2019. A review of 10 years of
572 human microbiome research activities at the US National Institutes of Health, Fiscal Years 2007-
573 2016. Microbiome 7, 31. https://doi.org/10.1186/s40168-019-0620-y.

574 Ratnesar-Shumate, S., Williams, G., Green, B., Krause, M., Holland, B., Wood, S., Bohannon, J.,
575 Boydston, J., Freeburger, D., Hooper, I., Beck, K., Yeager, J., Altamura, LA., Biryukov, J.,
576 Yolitz, J., Schuit, M., Wahl, V., Hevey, M., Dabisch, P. 2020. Simulated sunlight rapidly
577 inactivates SARS-COV-2 on surfaces. J Infect Dis. 222(2):214-222.
578 https://doi.org/10.1093/infdis/jiaa274.

579 Razzini, K., Castrica, M., Menchetti, L., Maggi, L., Negroni, L., Orfeo, N. V., Pizzoccheri, A.,
580 Stocco, M., Muttini, S., Balzaretti, C. M. 2020. SARS-CoV-2 RNA detection in the air and on
581 surfaces in the COVID-19 ward of a hospital in Milan, Italy. The Science of the total
582 environment, 742, 140540. Advance online publication.
583 https://doi.org/10.1016/j.scitotenv.2020.140540.

584 Segre, J.A. 2013. What does it take to satisfy Kochôs postulates two centuries later? Microbial
585 genomics and Propionibacteria acnes. J Invest Dermatol. 133(9), 2141ï 2142.

586 https://doi.org/10.1038/jid.2013.260

587 Slatko BE, Gardner AF, Ausubel FM. 2018. Overview of Next-Generation Sequencing
588 Technologies. Curr Protoc Mol Biol. 2018 Apr;122(1):e59. https://doi.org/10.1002/cpmb.59.

589 Somsen, G. A., van Rijn, C., Kooij, S., Bem, R. A., & Bonn, D. 2020. Small droplet aerosols in
590 poorly ventilated spaces and SARS-CoV-2 transmission. The Lancet. Respiratory medicine, 8(7),
591 658-659. https://doi.org/10.1016/S2213-2600(20)30245-9.

592 Stadnytskyi, V., Bax, C. E., Bax, A., & Anfinrud, P. 2020. The airborne lifetime of small speech
593 droplets and their potential importance in SARS-CoV-2 transmission. Proceedings of the
594 National Academy of Sciences of the United States of America. 117(22), 11875-11877.
595 https://doi.org/10.1073/pnas.2006874117.

596 Valeriani, F., Protano, C., Gianfranceschi, G., Cozza, P., Campanella, V., Liguori, G., Vitali, M.,
597 Divizia, M., Romano Spica, V. 2016. Infection control in healthcare settings: perspectives for
598 mfDNA analysis in monitoring sanitation procedures. BMC infectious diseases. 16, 394.
599 https://doi.org/10.1186/s12879-016-1714-9.

600 Valeriani, F., Agodi, A., Casini, B., Cristina, M. L., D'Errico, M. M., Gianfranceschi, G.,
601 Liguori, G., Liguori, R., Mucci, N., Mura, I., Pasquarella, C., Piana, A., Sotgiu, G., Privitera, G.,
602 Protano, C., Quattrocchi, A., Ripabelli, G., Rossini, A., Spagnolo, A. M., Tamburro, M., Romano
603 Spica, V., GISIO Working Group of the Italian Society of Hygiene, Preventive Medicine, and
604 Public Health. 2018a. Potential testing of reprocessing procedures by real-time polymerase chain
605 reaction: A multicenter study of colonoscopy devices. American journal of infection control.
606 46(2), 159ï 164. https://doi.org/10.1016/j.ajic.2017.08.008.

607 Valeriani, F., Crognale, S., Protano, C., Gianfranceschi, G., Orsini, M., Vitali, M., Romano
608 Spica, V. 2018b. Metagenomic analysis of bacterial community in a travertine depositing hot
609 spring. The new microbiologica, 41(2), 126ï 135.

610 Valeriani, F., Protano, C., Gianfranceschi, G., Leoni, E., Galasso, V., Mucci, N., Romano Spica,
611 V. 2018c. Microflora Thermarum Atlas project: Biodiversity in thermal spring waters and natural
612 SPA pools. Water Science and Technology: Water Supply. 18: 1472ï 1483.

613 Valeriani, F., Margarucci, L. M., Gianfranceschi, G., Ciccarelli, A., Tajani, F., Mucci, N.,
614 Ripani, M., & Romano Spica, V. 2019. Artificial-turf surfaces for sport and recreational
615 activities: microbiota analysis and 16S sequencing signature of synthetic vs natural soccer fields.
616 Heliyon, 5(8), e02334. https://doi.org/10.1016/j.heliyon.2019.e02334.

617 Van Doremalen, N., Bushmaker, T., Morris, D.H., Holbrook, M.G., Gamble, A., Williamson,
618 B.N., Tamin, A., Harcourt, J.L., Thornburg, N.J., Gerber, S.I., Lloyd-Smith, J.O., de Wit,E.,

619 Munster, V.J. 2020. Aerosol and surface stability of SARS-CoV-2 as compared with SARS-
620 CoV-1. N Engl J Med. 382, 1564-1567. https://doi.org/10.1056/NEJMc2004973.

621 Veronesi, L., Colucci, M.E., Pasquarella, C., Caruso, L., Mohieldin Mahgoub Ibrahim, M., Zoni,
622 R., Pergreffi, M., Arcuri, C., Seidenari, C., Viani, I., Capobianco, E., Mezzetta, S., Affanni, P.
623 2020. Virological surveillance of SARS-CoV-2 in an Italian northern area: comparison of Real
624 Time RT PCR cycle threshold (Ct) values in three epidemic periods.Acta Biomed. 2020 Jul
625 20;91(9-S):19-21. https://doi.org/10.23750/abm.v91i9-S.10138.

626 Wang, J., Feng, H., Zhang, S., Ni, Z., Ni, L., Chen, Y., Zhuo, L., Zhong, Z., & Qu, T. 2020.
627 SARS-CoV-2 RNA detection of hospital isolation wards hygiene monitoring during the
628 Coronavirus Disease 2019 outbreak in a Chinese hospital. International journal of infectious
629 diseases: IJID: official publication of the International Society for Infectious Diseases. 94, 103ï
630 106. https://doi.org/10.1016/j.ijid.2020.04.024.

631 Wei, L., Lin, J., Duan, X., Huang, W., Lu, X., Zhou, J., Zong, Z. 2020. Asymptomatic COVID-
632 19 Patients Can Contaminate Their Surroundings: An Environment Sampling Study. mSphere.
633 5(3), e00442-20. https://doi.org/10.1128/mSphere.00442-20.

634 WHO, World Health Organization. 2020. Transmission of SARS-CoV-2: implications for
635 infection prevention precautions. Scientific Brief. https://www.who.int/news-
636 room/commentaries/detail/transmission-of-sars-cov-2-implications-for-infection-prevention-
637 precautions (accessed 10 August 2020).

638 WHO, World Health Organization. Infection Prevention and Control of Epidemic-and Pandemic-
639 prone Acute Respiratory Infections in Health Care. Geneva: World Health Organization; 2014
640 https://apps.who.int/iris/bitstream/handle/10665/112656/9789241507134_eng.pdf;jsessionid=41
641 AA684FB64571CE8D8A453C4F2B2096?sequence=1 (access 10 August 2020).

642 Wu, S., Wang, Y., Jin, X., Tian, J., Liu, J., Mao, Y. 2020. Environmental contamination by
643 SARS-CoV-2 in a designated hospital for coronavirus disease 2019. American journal of
644 infection control. 48(8), 910ï 914. https://doi.org/10.1016/j.ajic.2020.05.003.

645 Yao, T., Han, X., Guan, T., Wang, Z., Zhang, S., Liu, C., Liu, C., Chen, L. 2020. Effect of
646 indoor environmental exposure on seminal microbiota and its application in body fluid
647 identification. Forensic science international. 314, 110417. Advance online publication.
648 https://doi.org/10.1016/j.forsciint.2020.110417.

649

650

Table 1

Classification / ***Surface source***	***Samples***	**Dataset (N=94)**	**Description**	**Nucleic Acid Testing**		
				SARS-CoV-2	Biofluid (RT-PCR)	Microbiota (NGS)
Indoor	***Hospital***	**49**	Floor (n=7)	+	+	+
			Bedside table (n=3)	+	+	+
			Door handle (n=3)	+	+	+
			Call button (n=1)	+	+	+
			Table (n=1)	+	+	+
			Chair (n=2)	+	+	+
			Back of the bed (n=3)	+	+	+
			Side of bed (n=4)	+	+	+
			Bottom of the bed (n=1)	+	+	+
			Wall behind the bed head (n=1)	+	+	+
			Bed sheets (n=1)	+	+	+
			Pillow (n=2)	+	+	+
			Stethoscope (n=1)	+	+	+
			Wheelchair head (n=1)	+	+	+
			Toilet board (n=1)	+	+	+
			Toilet flush button (n=1)	+	+	+
			Sink faucet (n=1)	+	+	+
			Air circulation system (15)	+	-	-
	Public Building	**25**	Door handle (n=2)	±	+	+
			Toilet (n=2)	+	+	+
			Pews (n=4)	-	+	+
			Floor (n=6)	±	+	+
			Toilet wall tiles (n=3)	±	+	+
			Office phone (n=1)	+	+	+
			Computer keyboard (n=2)	+	+	+
			Air circulation system (n=5)	-	+	+
Outdoor		***16***	Handrail (n=1)	+	+	+
			Grip shared e-scouter (n=1)	+	+	+
			Bus stop bench (n=1)	+	+	+
			Coffee dispenser button (n=1)	+	+	+
			External door handle (n=2)	±	+	+
			Playground (n=10)	-	±	+
Human		***4***	Droplets◊biofluid (n=4)	±	+	+

651

652 **Table 1. Environmental sampling: dataset of collected samples and testing.** Indoor surfaces were
653 sampled from different hospitals (n=3), buildings of public use (1 office, 1 Fast food, 1 church), outdoor
654 areas (n=16), nose-oropharyngeal secretions (n=4) and tested for presence of SARS-CoV-2 and for
655 anthropic contamination by testing the presence of microbiota traces of biological fluids (Nose, Saliva,
656 Feces), by Real Time PCR (RT-PCR) and/or Next Generation Sequencing (NGS). For each type of test,
657 analysis was performed in all (+), no one (-) or some (±) of the collected samples.

658
659

Table 2

ANTROPIC CONTAMINATION FROM BIOFLUIDSô MICROBIOTA

			Droplets			
Sample source	***Code***	***Skin***	***Nasopharynx***	***Oropharynx***	***Feces***	***Sample description***
Controls (n=4)	**A_01**	-	+++	-	-	Dropletsô biofluid
	A_02	++++	+++++	+	-	Dropletsô biofluid
	A_03	++++	+++++	++	-	Dropletsô biofluid
	A_04	++++	++++++	+	-	Droplets ô biofluid
Outdoor (n=6)	**Z_01**	+++	+++	-	+	Handrail
	Z_02	+/-	+	-	-	Bus stop bench
	Z_03	++	++	-	+/-	Shared e-scouter grip
	Z_04	-	+	-	-	External door handle
	Z_05	++	+	-	+/-	External door handle
	Z_06	++	+	-	-	Coffee dispenser
Indoor (n=55)	**YH1_01**	+++	++	+	+	Right bed rail*
	YH1_02	+++	++	+/-	+/-	Bedside table
	YH1_03	++	+++	++++	+++	Door handle
	YH1_04	++	+++	-	+/-	Floor
	YH1_05	++	++++	+	+++	Call button*
	YH1_06	++	++	-	-	Table
	YH1_07	-	++	-	-	Chair
	YH1_08	-	+++	-	-	Back of the bed
	YH1_09	-	++	-	-	Air inlet socket
	YH1_10	+++	++	+++	-	Wall behind the bed
	YH1_11	+++	+++	+++	++	Left bed rail
	YH1_12	-	+++	-	-	Stethoscope*
	YH1_13	-	+++	-	-	Bottom of the bed
	YH1_14	+	++++	-	+/-	Wheelchair head
	YH2_15	++++	++	-	-	Pillow
	YH2_16	-	+	-	-	Chair
	YH2_17	-	+	-	-	Back of the bed
	YH2_18	-	+/-	-	+/-	Toilet board
	YH2_19	-	+/-	-	+	Sink faucet
	YH2_20	-	++	-	-	Floor
	YH2_21	+	+/-	-	-	Floor
	YH2_22	-	++	++++	-	Floor
	YH2_23	-	+	-	-	Door handle
	YH2_24	+++	++	-	+/-	Back of the bed
	YH2_25	++	+	++++	-	Side of bed
	YH2_26	+	+	-	+++	Side of bed
	YH2_27	-	-	-	-	Bedside table
	YH2_28	-	+/-	-	+	Bedside table

			Droplets			
Sample source	***Code***	***Skin***	***Nasopharynx***	***Oropharynx***	***Feces***	***Sample description***
	YH2_29	-	++	-	-	Pillow
	YH2_30	-	+	-	-	Bed sheets
	YH2_31	+	++	-	-	Floor
	YH2_32	-	++	-	-	Floor
	YH2_33	-	+	-	-	Floor
	YH3_34	++++++	++++	-	-	Toilet
	YH3_35	-	++	-	-	Toilet
	YH3_36	+/-	-	-	-	Door handle
	YC_37	-	+	-	-	Pew and surface
	YC_38	-	+	-	-	Pew and surface
	YC_39	-	+	-	-	Pew and surface
	YC_40	++	++++	+	-	Pew and surface
	YO_41	-	-	-	+	Floor
	YO_42	-	-	+/-	+/-	Floor
	YO_43	-	-	-	+	Floor
	YO_44	-	-	-	+	Floor
	YO_45	-	-	-	-	Floor
	YO_46	-	-	-	+	Floor
	YO_47	-	-	-	+/-	Toilet wall tiles
	YO_48	-	-	-	+	Toilet wall tiles
	YO_49	-	-	-	+	Toilet wall tiles
	YO_50	-	-	-	+/-	Office phone
	YO_51	-	-	-	+	Computer Keyboard
	YO_52	+/-	-	-	+	Computer Keyboard
	YO_53	+	+	+	+	Elevator handle
	YO_54	+++	+++	+	+/-	Toilet door handle
	YO_55	++	++	-	-	Toilet flush button

Table 2. Anthropic contamination by Real Time PCR. The cumulative output of indicators for each anthropic contamination is shown, including the description of each sample. For each indicator: ñ+++ò Positive: Ct <20; ñ++ò Positive: Ct 20-30; ñ+ò Positive Ct 30-35; ñ+/-ò Doubt: Ct 36-38; ñ-ò Negative Ct >39. For *E. faecalis*: ñ++ò Positive: Ct <20; ñ+ò Positive Ct 21-29; ñ+/-ò Doubt: Ct 30-35; ñ-ò Negative Ct >36. The asterisk (*) shows the sampling points where SARS-CoV-2 RNA was detected. Sample reading code: A: anthropic, Z: outdoor; Y: indoor (H: hospital; C: church; O: office and restaurant).

669 **Table 3**

670

671

672

RT-PCR Droplets' Markers				
Origin	**Indicators**	***RC1***	***RC2***	***RC3***
Nasopharynx	*Propiniumbacterium spp*	**0.93**	0.05	-0.01
	Corynebacterium spp	**0.66**	-0.03	0.39
Oropharynx	*Streptococcus mutans*	0.21	**0.76**	0.11
	Staphylococcus salivarius	0.02	**0.89**	-0.15
Nostril-skin	*Staphylococcus aureus*	0.06	0.30	**0.80**
	Staphylococcus epidermidis	0.13	-0.07	**0.88**

673

674

675

676

677

678

679

680

681

682 **Table 3. Primary indicators for droplets.** Pattern matrix for principal component analysis
683 nasopharynx selected indicators *(Propiniumbacterium spp.*, *Corynebacterium spp.)*, oropharynx
684 *(Streptococcus mutans*, *Staphylococcus salivarius*), of nostril-skin (*Staphylococcus aureus*,
685 *Staphylococcus epidermidis).* The higher correlations for each component (RC) are shown in bold
686 ($p<0.01$). The table reported variable loading on the rotation matrix.

687

688 **Figure 1**

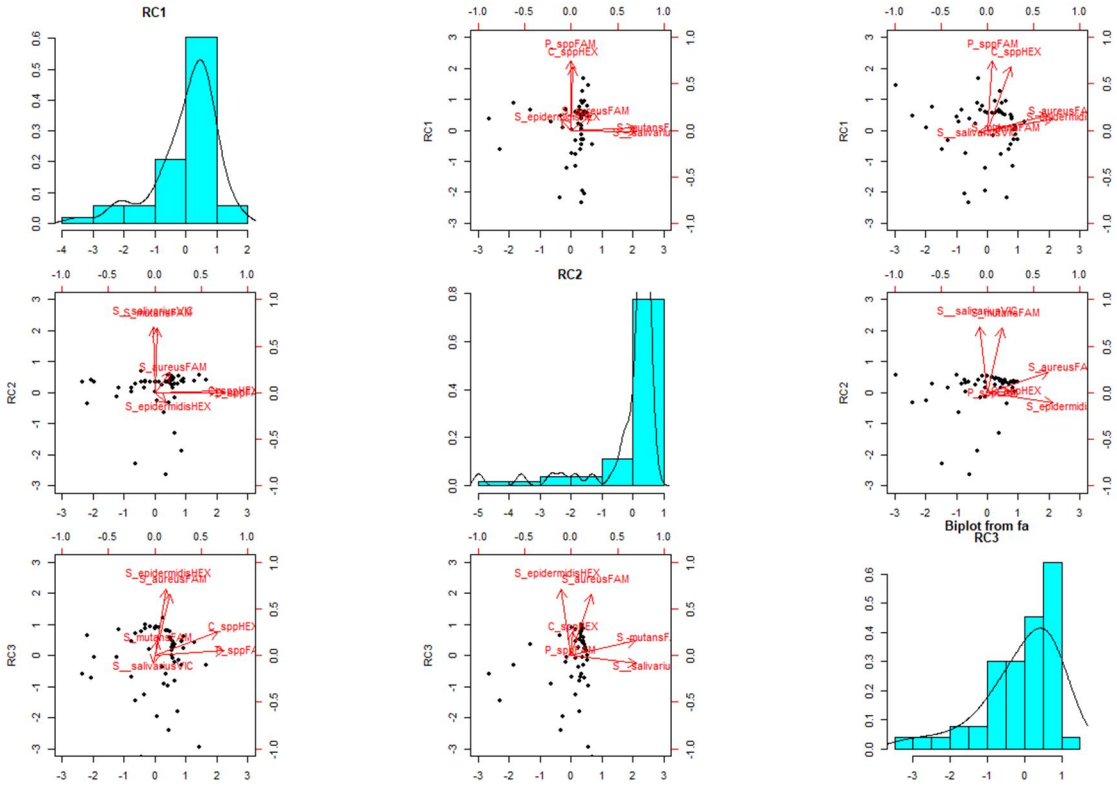

689

690

691

692

693

694 **Figure 1. Dropletsô componentsô distribution.** Principal Component Analysis biplots showing
695 Component 1 versus Component 2, Component 1 versus Component 3 and Component 2 versus
696 Component 3. The first, second, and third component explain 28%, 27%, and 27% of the variability
697 observed, respectively. The role of the bacterial indicators within the different components is
698 summarized by vectors within the scatter graphs.

699

700 **Figure 2**

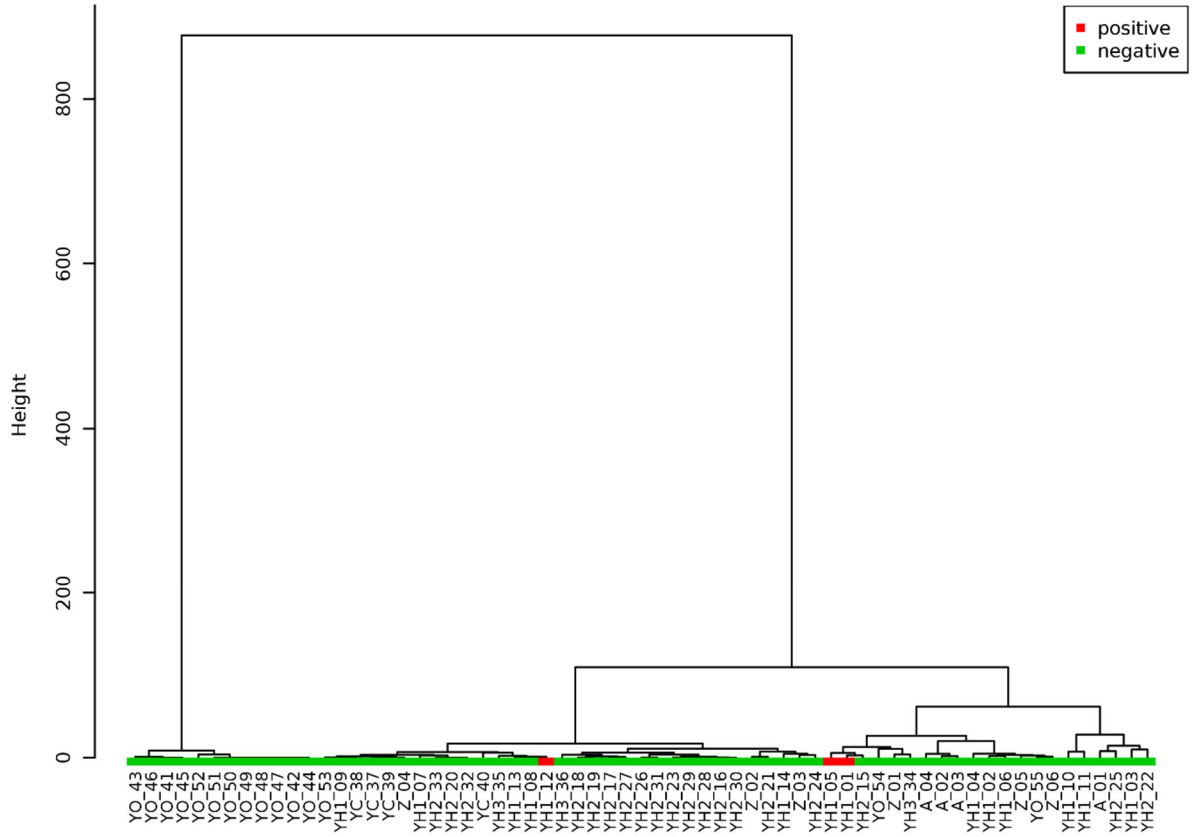

701

702

703 **Figure 2. Hierarchical cluster analysis on Real Time PCR results.** SARS-CoV-2 positive and
704 negative samples are indicated in green and red, respectively. The hierarchical cluster was
705 performed on raw CT data by Euclidean distance and Ward's linkage (clustering to minimize the
706 sum of squares of any two clusters).

707

708 **Figure 3**

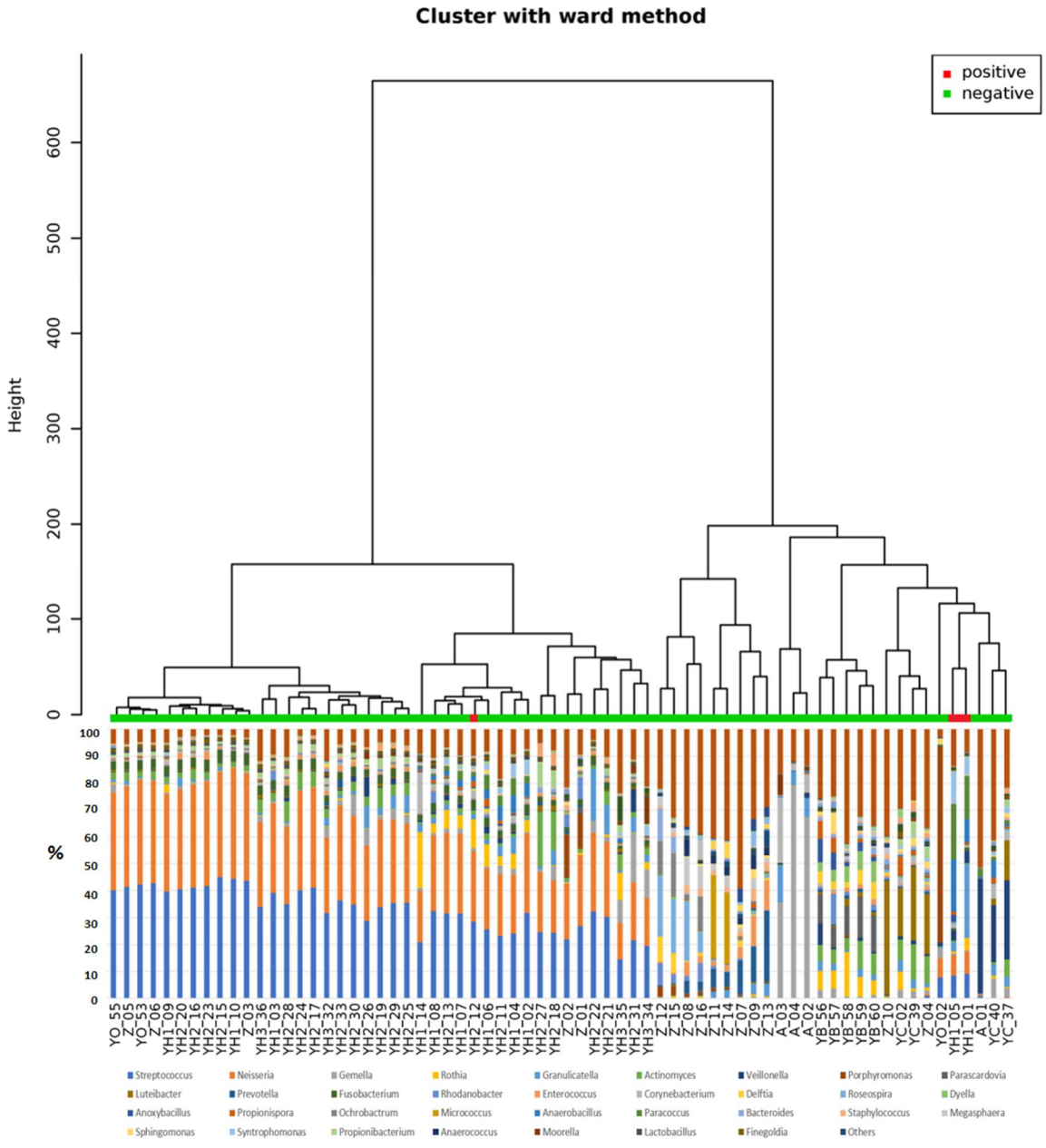

709

710

711 **Figure 3. Hierarchical Clustering Dendrogram on 16S amplicon sequencing data.**
712 Dendrogram shows a hierarchical clustering of samples based on genus-level classifications. The
713 bar chart under each sample summarizes the relative abundance of its genus-level classifications.
714 In this analysis were included also environmental samples from playgrounds (Z_07-16) and indoor
715 air (YB_56-60), without major anthropic contaminations. SARS-CoV-2 negative and positive
716 samples are indicated in green and red, respectively.

717

718 **Figure 4**

719

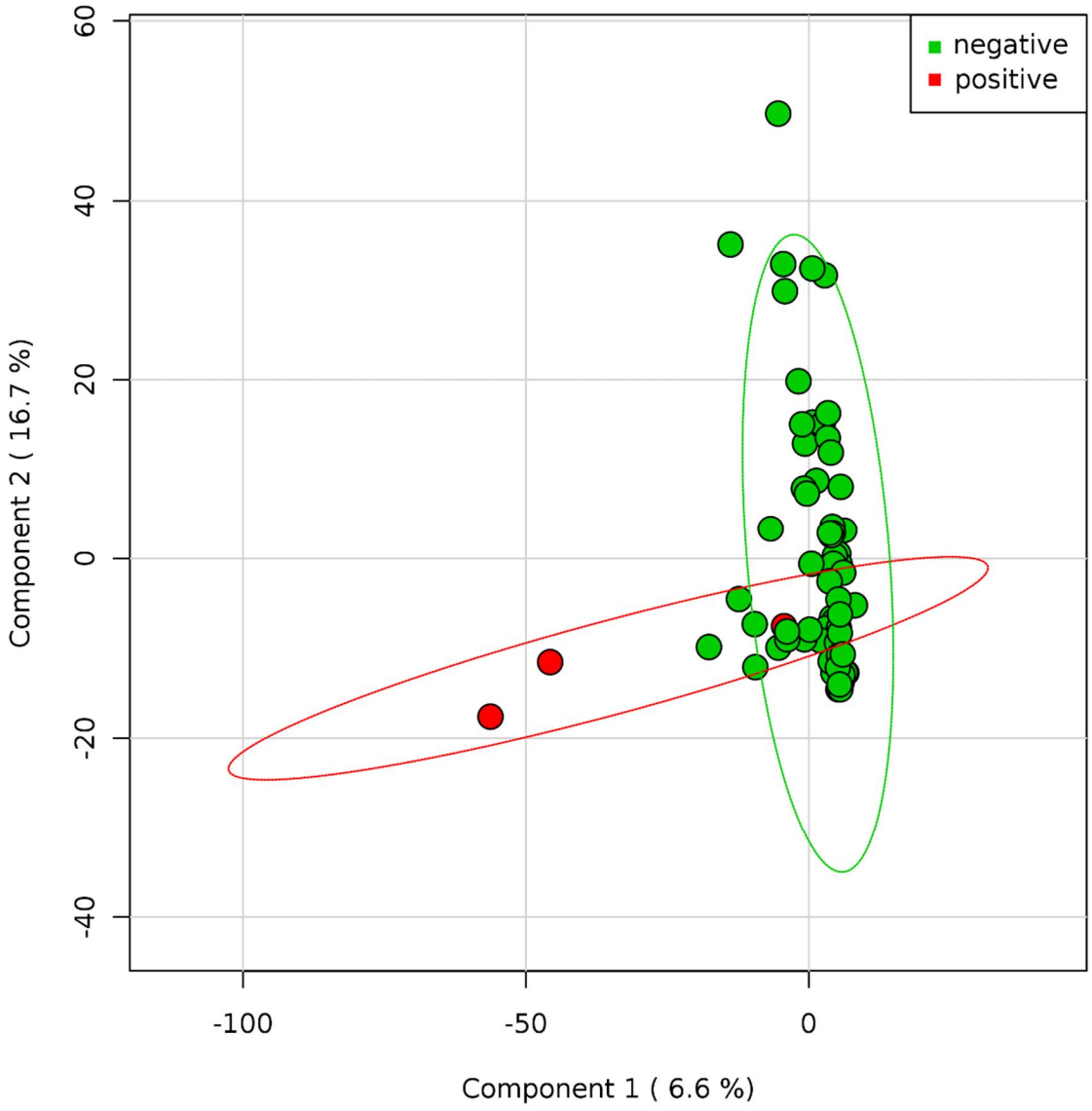

720

721

722 **Figure 4. SARS-CoV-2 positive and negative samples.** Principal Coordinate Analysis of the
723 normalized relative abundance of all samples divided by negative and positive results of SARS-
724 COV2. Data are plotted at the genus-level classification. The variance is explained for 6.6% and
725 16.7%, respectively for Component 1 and 2. SARS-CoV-2 positive (red) and negative (green)
726 samples.

727

728 **Figure 5**

729

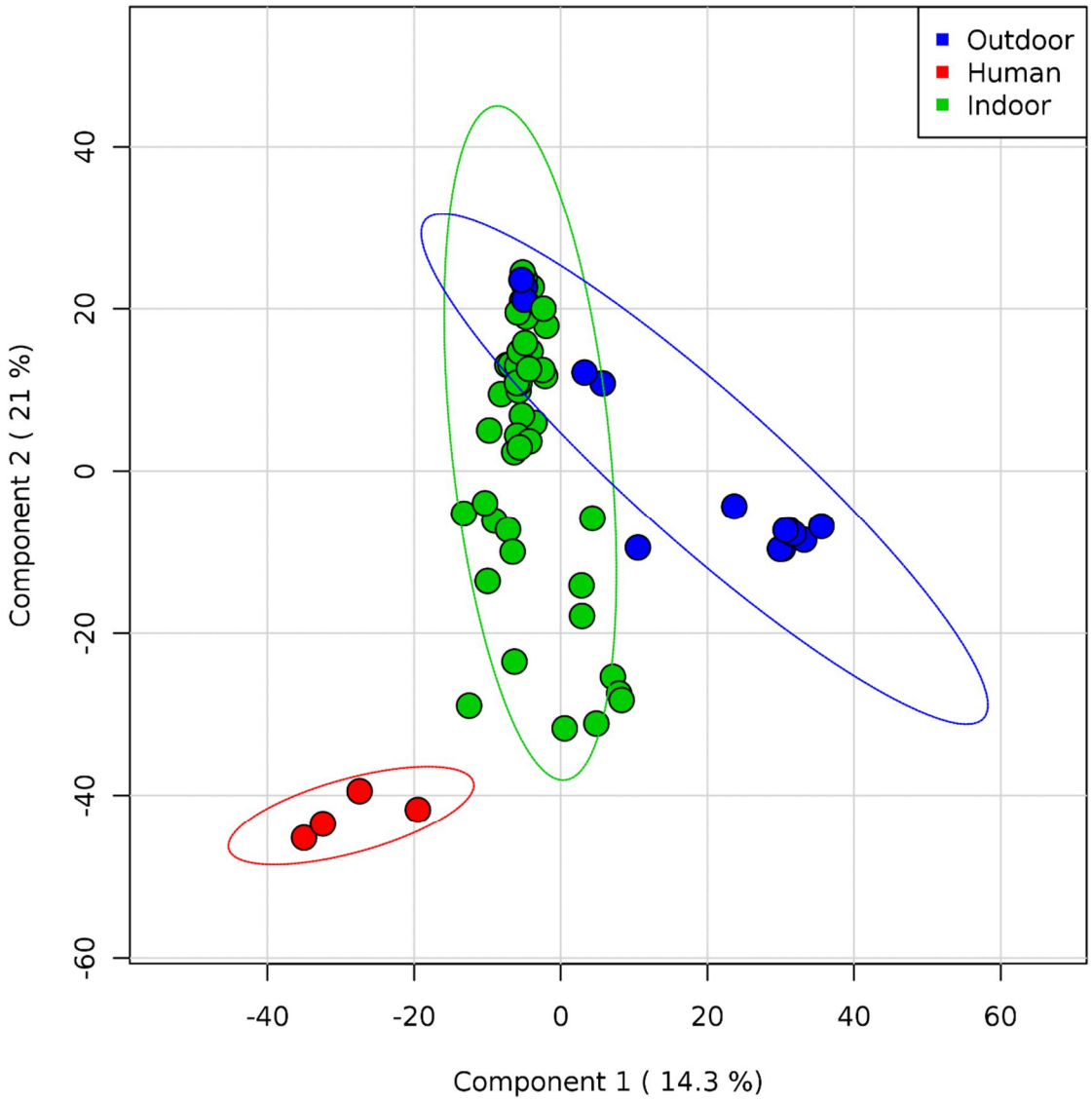

730

731 **Figure 5. Whole microflora analysis of indoor and outdoor samples.** Partial least square-
732 discriminant analysis (PLS-DA) shows Pearson distance between different samples using
733 phylogeny distribution based on 16S rRNA genes. Samples are colored according to the sampling
734 point (red: human droplets; green: indoor; blue: outdoor). The variance is explained for 14.3 %
735 and 21 %, respectively for Component 1 and 2. Outdoor samples overlapping indoor samples are
736 characterized by fomites, whereas the blue sample between groups is the outdoor handle of a
737 building main entrance. All samples without a major presence of environmental microflora, but
738 characterized by a prevalence of human microbiota from droplets biofluids, tend to segregate
739 independently.